A review of time domain impedance boundary conditions

C. Richter

Rolls-Royce Deutschland LTD & Co. KG, Eschenweg 11, Dahlewitz, 15827 Blankenfelde-Mahlow, Germany
christoph.schemel@web.de

Over the last 15 years, time domain impedance boundary conditions have been investigated by various authors. In a review, a general framework of time domain impedance boundary conditions is presented and then filled with a set of outstanding mathematical and numerical methods from literature. All of the authors struggled with an instability with grazing flow. Mainly this is linked to the Ingard or Myers model of the sound propagation through a sheared flow. This is reviewed in a broader context including possible applications of impedance boundary conditions (i.e. turbomachinery noise and noise absorber optimization) into this discussion. Stable solutions are presented, that go from simple workarounds which are based on the wave number characteristics of the instability to a completely different modeling of the physics. At one end of the scale are seemingly trivial ideas, as the use of the Ingard/Myers boundary condition on a coarser mesh or a fully resolved flow profile; and at the other end high fidelity DNS simulations of single cells and holes under gazing flow conditions is put the whole idea of macroscopic impedance on test. It is shown, that each solutions has its advantages for some applications and may be infeasible in other cases.

1 Introduction

Today, besides source noise reduction, the passive acoustic treatment of the internal path of noise in the aeroengine is still the standard technique to achieve noise reduction objectives. The best ratio between weight and noise reduction is currently still achieved by generalized Helmholtz resonator or quarter wavelength panels as the one sketched in Figure 1. These panels feature at least three basic design elements; a rigid back plate, a defined acoustic resistance and a cavity, that provides a phase shift of the liner reaction to the incoming wave. In the schematic figure below the resistance to dissipate the acoustic wave is provided by a perforate plate with holes or a mesh. Bulky materials would combine the phase shift and the resistance in one material. However, they are not so frequently used for aeroengines.

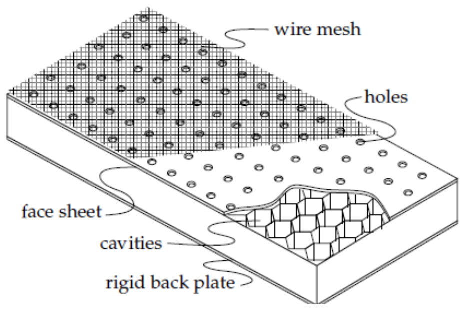

Figure 1: Schematic of an acoustic liner for turbomachinery noise.

Due to an increasingly high demand for aircraft noise reduction, the passive acoustic treatments enter new areas in the aeroengine. The prediction of the liner attenuation in most of these areas is only possible with the help of numerical methods, because either they are close to a noise source and non-linear effects dominate the pressure and velocity field or the geometric and flow situation is complex.

On the other side, numerical methods have successfully gained acceptance in all fields of industrial research and development, such that their application for the liner problem seems to be in reach. Novel methods for accurate and cost-efficient description of unsteady flow phenomena become more and more used in industrial applications and Numerical methods for the computation of specific aeroacoustic phenomena have been greatly developed over the last two decades. These methods can exhibit important achievements for all the issues that are relevant to the aeroacoustics of an aeroengine. The sound propagation inside the engine ducts and to the moderate far field is efficiently predicted by high-order schemes for computational aeroacoustic problems in the time domain. The impedance modeling is one of the major issues to complete this development.

The current paper reviews the progress of numerical impedance modeling. Especially in the last 15 years, Impedance models in the time domain have seen a fast progress but also limitations of the modeling have been uncovered. These are presented in short here, to give an introduction and advice for the application of such models with CFD (source) or CAA (propagation and near field radiation) methods. This is done in the second part of the paper. Almost as important as the numerical boundary condition itself are the input parameters that describe a liner, which can be made in real engine hardware. Therefore the first part of this paper reviews the available methods to measure impedance. Fully numerical approaches to calculate the impedance and develop novel liner models, which will be based on a direct numerical simulation (DNS) are touched as well. Finally conclusions are drawn on the application of impedance models and numerical methods for turbomachinery noise attenuation prediction and understanding.

2 The Acoustic Impedance

Thinking straight forward, the performance of an acoustic liner would be best described by its sound absorption. For aero engines, the acoustic liner is typically placed at the walls of a duct and the sound waves propagate along this wall parallel or opposite to a grazing flow. In this situation, the insertion loss seems to be a good measure of the acoustic performance. It is defined as the difference in sound power between hard wall and acoustically treated duct, which is measured at the duct end away from the noise source. However, the insertion loss depends on frequency and sound source as well as the grazing flow and other potential parameters of influence.

The above definitions attempt to provide a relation between measurable (i.e. geometric) parameters of the acoustic treatment and the performance of the absorber via a measurement. However, the exact measure of the liner performance requires a measurement under the exact source conditions (magnitude, modal angle, etc.), base flow and geometric situation. So insertion loss is not considered as a good measure.

Better suited seems to be the acoustic impedance, which describes the local properties of the wall for the acoustic waves. The acoustic impedance is defined in the frequency domain as:

$$Z(i\omega) = \frac{\hat{p}(i\omega)}{\hat{u}_n(i\omega)} \quad (1)$$

where $Z(i\omega)$ denotes the complex impedance and p and u the complex pressure and normal velocity magnitudes. The impedance provides a frequency dependent ratio of pressure and normal velocity at the absorber surface. This allows compensating for different modal angles between measurement and application source noise. The parallel velocity component has to fulfill either a no slip or slip condition, whereas the normal component fulfills the impedance boundary condition in an analytical or numerical approach.

The use of acoustic impedance makes the required measurement independent of the geometry. With a valid model, other effects may be added, such that the requirements for a valid measurement of the impedance are much lower than for insertion loss. Finally the use of the acoustic impedance eases the optimization and modeling of a lined surface, because it allows including various effects via a model, instead of being fixed to a direct measurement with a real liner.

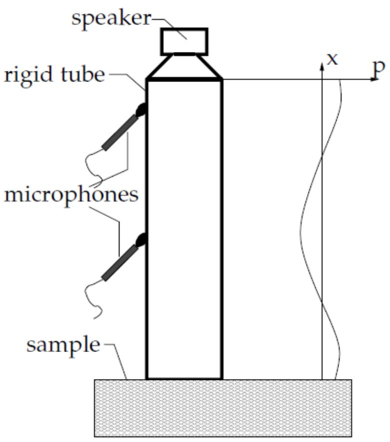

Figure 2: Schematic impedance measurement without grazing flow with Kundts tube (portable commercial solutions available)

To name only one of such models, the model of Ingard [1] for the conservation of the acoustic particle displacement over an infinite thin shear layer at the liner surface is given:

$$\hat{u}_n(i\omega) = \frac{\hat{p}(i\omega)}{Z(i\omega)} + \boldsymbol{u}_0 \cdot \nabla \left(\frac{\hat{p}(i\omega)}{i\omega\, Z(i\omega)} \right) \quad (2)$$

It was extended by Myers for arbitrary curved surfaces.

3 Ways to Measure Impedance

The use of the acoustic impedance makes it now necessary to obtain the acoustic impedance from measurements. In the following a short overview on the different methods to measure impedance shall be given. Some limitations of the methods are given as well.

3.1 Kundts Tube Without Flow

The principle of Kundts tube allows to calculate the impedance of a surface from the standing wave pattern in a tube. The standing waves are excited with a speaker. The method is based on plane wave propagation in the tube and therefore limited to frequencies below the cut-on frequency of the first higher mode in the tube. The tube diameter and microphone distance determine the measurement range of the tube.

With some potential drawback on measurement repeatability and accuracy, this method even allows the non-destructive measurement of impedance with a portable device. This method cannot however, directly be extended to a measurement with grazing flow.

3.2 Insertion loss, Reflection & Transmission

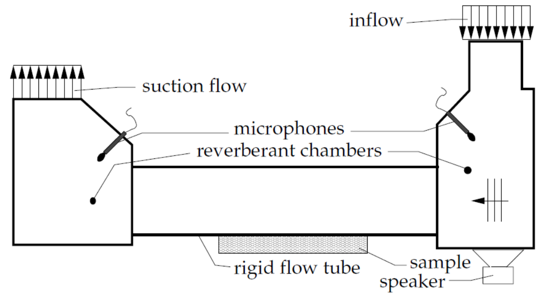

Figure 3: Impedance measurement in a flow tube setup (wind tunnel e.g. [2])

The principle shown in Figure 3 implements the direct measurement of the transmission loss with two reverberant chambers in a wind tunnel. The chambers are required to integrate the sound intensity over the duct diameter. The measurement can be taken with flow. Due to the different absorption characteristics of different modes, the method allows only accurate back calculation of the impedance from the measurements below the cut-on frequency of the first higher mode in the duct.

This back calculation can be based on numerical methods (see below) or analytical approaches, which provide the transmission loss. With the knowledge of the modal content in the duct, the impedance back calculation may be extended to higher frequencies for this method. However, the measurement and computation effort increases drastic with more and more modes getting cut-on.

3.3 Exponential Decay of Pressure Amplitude

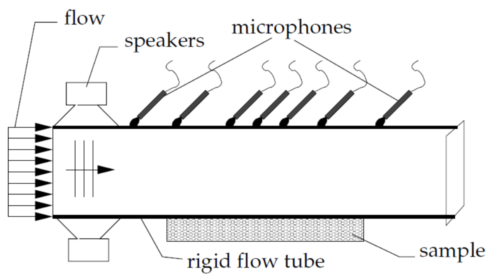

Figure 4: Impedance measurement in a flow tube setup with microphones opposite to the sample ([4][5][6][7][8] etc.)

This method provides a measurement of the exponential decay of the pressure at the wall opposite to the liner. If only one mode is cut-on in the lined duct, the solution with liner can be described as $p \sim exp(ikx)\, exp(-\alpha x)$, where k and α are real constants and α is positive. The constant α depends on frequency and impedance of the wall only, such that the measurement of the exponential decay and a curve fit can be used to determine the impedance. The set up for such measurement is shown schematically in Figure 4.

3.4 Hybrid methods

The measurement of insertion loss, transmission and reflection are often combined in a single set up, or microphones at the opposite wall up-and downstream of the sample are used instead of reverberant chambers to calculate the transmission and reflection [7]. The application of the resulting data for impedance back calculation is the same as above, it simply provides more redundant information to the methods.

3.5 In Situ Measurement

A special method for the almost direct measurement of the acoustic impedance was developed by NLR [9]. It uses microphones in the liner cell to provide a measurement of the standing wave pattern and the incoming acoustic field. With two microphones, this measurement allows then a very accurate calculation of the impedance under grazing flow conditions directly at the liner surface. The method is not limited to conditions without flow, but in principle very similar to a Kundts tube measurement. However the method is intrusive and requires instrumentation in the cells of the liner.

3.6 Impedance Eduction with CAA Methods

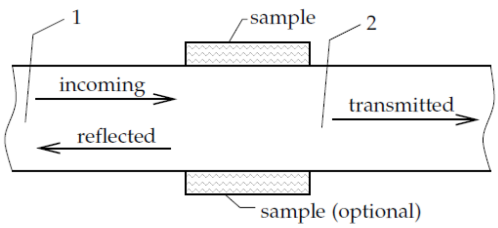

Figure 5: Model for the impedance eduction with CAA methods [7]

Finally, the back calculation of the impedance from measurements shall be outlined, as it is one of the key techniques for the development of impedance models and the fit of such models to existing data.

In the last years, many impedance boundary conditions for time domain CAA codes have been reported [12][13][14][15][16][17][18]. With these boundary conditions, there is a growing need to provide model parameters for specific liner hardware. Impedance eduction from measurements with such a model is one of the straight forward methods to firstly obtain the model parameters and secondly get an accurate time domain impedance boundary condition for further predictions.

Such an impedance eduction is also reported by more and more authors using different time domain or frequency domain impedance models [4][5][11][7][8].

3.7 Calculation with DNS / LES

Finally, a purely numerical method to calculate the impedance is provided by DNS methods. This way was first applied by Tam for a slit resonator. Today e.g. Zhang has presented very promising DNS results for a single hole over a cavity without [20] and with flow [21].

The impedance calculation for a Helmholtz resonator is a complex numerical multiple scales problem. The scales range from the acoustic wave length and the cavity depth (in the order of several centimeters inch or more) over the boundary layer profile of the main flow, the hole diameter and thickness of the facing sheet, which both can be in the order of millimeters down to the boundary layer in these small holes. The disparity of length scales (i.e. the acoustic wavelength and resolution for the boundary layer profile in the orifice) leads to a large variability of time scales as well. Especially the boundary layer inside the hole and the jets from the hole with small scale structures are crucial to compute the correct resistance for a liner. For an explicit scheme, as it is frequently used in DNS, the time step size is determined by the smallest cells (in the boundary layer inside the hole). On the other hand for a full acoustic period, a relatively large time series is required. Altogether, this makes the direct numerical simulation of an acoustic liner a complex problem which requires high computation effort.

Currently DNS methods are only applied for single liner cells or even single orifices. Even for these small problems require massive parallel computations on a super computer with a large number of CPUs. While this effort seems reasonable for simulations that improve the understanding for impedance modeling, DNS methods are far from being integrated into a simulation of turbomachinery components with a large number of orifices and liner cells.

DNS simulations of orifices under grazing flow conditions might also provide a completely new understanding of impedance with grazing flow, which is based on the interaction of the boundary layer of the main flow with the acoustic boundary layer and jet. This understanding might in the near future replace the Myers boundary condition and provide a stable model for the impedance under grazing flow conditions, which is able to describe the full interaction and not only the convective components. As DNS works in the time domain, these models will not need the transform to the frequency domain and back. DNS will also help the understanding of interaction phenomena between orifices and non-linear effects.

4 Impedance Boundary Conditions

4.1 Time Domain Impedance Boundary Conditions

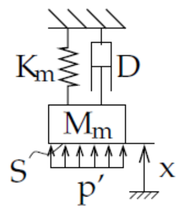

Figure 6: Mass-Spring-Damper analogue.

The development of time domain impedance boundary conditions from the beginning in 1996 showed two parallel approaches [12][13]. One of these streams relies on a physical motivated model for the impedance. This was started by Tam [12] with his mass-spring-damper based time domain impedance boundary condition:

$$Z=p/u_n=i\omega\, m + R + k/i\omega$$
$$\leftrightarrow \partial u_n/\partial t = m^{-1}(p + R\, u_n + k \int u_n\, dt) \quad (3)$$

The extended Helmholtz resonator model of Rienstra [17] with implementations like presented by Chevegaun [18] or Richter [10] falls into the same category. These formulations require a storage variable at the impedance wall, which allows a reflection of sound waves from the back sheet of the liner to be included in the model in terms of data from an earlier time step (i.e. cot(ikH) corresponds to $\delta(t + 2H/c)$ in the time domain). Common for these models is the presence of a mass reactance term ($i\omega\, m$), which is used to couple the ODE, that is solved for the impedance of the wall, to the linearized Euler equations (or similar formulations). In the reported implementations of the extended Helmholtz resonator model or the mass-spring-damper m cannot be zero therefore and it is reported, that small values of m lead to a stiff system and limit the maximum stable time step size.

The other way to formulate a time domain impedance boundary condition relies on the a multipole representation of the impedance, which puts back the physical understanding of the wall impedance in favor of the possibility to fit an almost arbitrary frequency response of the impedance. Such models were first presented by Ju and Fung [16] and later by many other authors. The impedance is represented as complex polynomial fraction, which corresponds to a pole of the impedance in the complex plane. For each of these poles only one additional variable is required, such that the number of storage variable is limited to the number of poles of the multipole formulation.

4.2 Grazing Flow Models

The boundary condition of Myers [2] can be written as:

$$\hat{u}_n(i\omega) = \frac{\hat{p}(i\omega)}{Z(i\omega)} \underbrace{+ u_0 \cdot \nabla \left(\frac{\hat{p}(i\omega)}{i\omega\, Z(i\omega)} \right)}_{\text{convective term}} \underbrace{- \frac{\hat{p}(i\omega)}{i\omega\, Z(i\omega)} n \cdot (n \cdot \nabla\, u_0)}_{\text{curvature term}} . \quad (4)$$

It describes the sound propagation through an infinitely thin shear layer under a conservation of the particle displacement over the shear layer, which is oriented locally parallel to an arbitrary curved surface. The surface curvature is also accounted in the convective correction. It should be noted that the sound propagation from a semi-infinite cylindrical duct through an infinite thin shear layer as it was described by Munt uses a similar model.

Several authors, who employ an impedance boundary condition under nonzero meanflow conditions, report an instability in their simulations. The instability is found in both time-domain and frequency-domain formulations. Only Ju and Fung considered the instability, which is observed by them only with a refined mesh as a purely numerical problem. All other authors, including Tester who first reported the problem, address it as a model-inherent instability of a Kelvin–Helmholtz type. The Ingard/Myers boundary condition provides a model for a free shear layer, which is necessary to support the Kelvin–Helmholtz instability. The shear layer model describes a dissipative effect, which adds rotation and non-isentropy to the base flow. This is the energy source for the instability, which may grow spatially or temporally without bounds in the linear model.

To further isolate the problem, it is necessary to look at the conditions under which the instability was revealed:

- A nonzero mean flow is necessary for the instability.
- Resolving the shear layer removes the instability in most cases.
- Some of the authors report the instability only for refined meshes, so the wavelength of instability must be smaller than the acoustic wavelength.
- If the discretization of the convective term is dissipative or implicit or a filter is applied, the instability is likely to be removed.

The analysis of Rienstra [23] considers the limit for large angular frequencies in combination with an infinitely thin shear layer at the surface. For this limit, the instability is always present, independently of the actual impedance and flow conditions [23]. A refined analysis of the surface waves and the connected instability is provided in the work of Brambley and coauthors [22]. They found that some of these surface waves may not be present for higher azimuthal modes m and a Helmholtz number built with the outer radius of the duct in the range of m. Rienstra and Vilenski recently also provide an extended analysis which uses a tanh-profile as template for the boundary layer. They show that the instability may be removed in the presence of a boundary layer of finite thickness. The presence of the instability is found to be depending on the momentum thickness of the boundary layer, the flow Mach number, the impedance and the excitation frequency. The result provides an insight under which conditions the instability becomes present. However, it does not remove the instability of the Myers boundary condition.

Brambley [22] suggests a method to remove the instability, which is based on the idea of a finite membrane stiffness. This clearly contradicts the idea of a locally reacting surface. This leads to an additional term, scaling with a fourth power of the wave number k, in the impedance model. However, this term becomes important for large k for which a finite difference approximation of the fourth derivative becomes most inaccurate. Therefore, adding the k^4-term suggested in [24] does not remove the instability in a preliminary study with the CAA method described in this thesis. Altogether, the latest analysis shows that the instability is present under realistic flow conditions for specific choices of impedance and flow parameters.

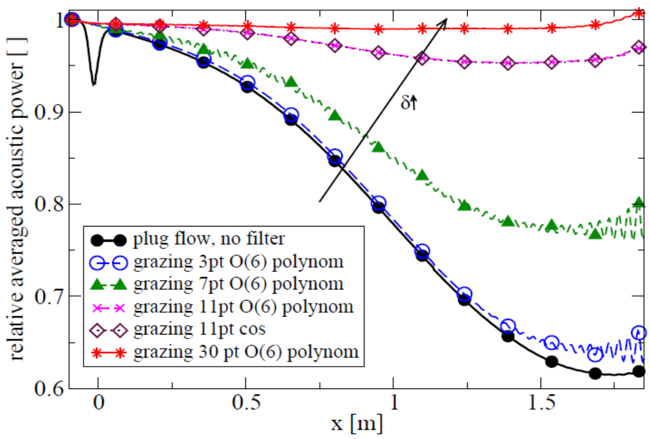

Figure 7: Comparison of grazing flow model and resolved boundary layer profiles in an intake duct (TUBA).

Possible ways to remove the instability seem to be the following approaches:

- A resolved boundary layer, which by the way provides a more accurate solution in case of a finite boundary layer thickness, especially when considering the propagation of sound waves against the flow with a significant boundary layer thickness compared with the acoustic wavelength (Figure 7).

- Low mesh resolution in combination with a filter that suppresses low wavelength components.
- A filter or dissipation, which is added to the convective and curvature terms (Figure 8).
- Development of entirely new models for the interaction of grazing flow boundary layer and acoustic waves based on DNS simulation.

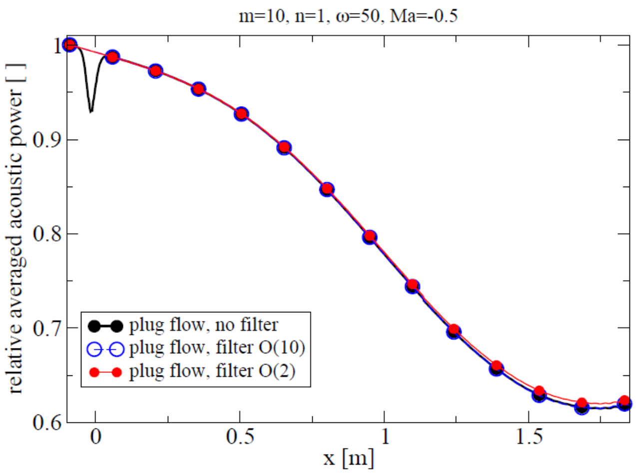

Figure 8: Comparison of pure and stabilized grazing flow models in an intake duct (TUBA).

The resolved mean flow profile is straight forward to implement with any CAA code solving the linearized Euler equations or a similar set of equations that is able to include the refraction of a shear layer. Figure 7 compares a resolved boundary layer profile of finite thickness to the boundary condition of Myers for an intake duct geometry with propagation of a m=10 mode against the flow at Ma=0.5. As no stabilization is applied, the solution with Myers boundary condition is unstable (the instability develops from the source region seen already as a dip in the solution). With increasing shear layer thickness, the attenuation significantly deviates from the solution with infinite thin shear layer assumption, which is due to the refraction away from the liner. With the shear layer thickness converging to zero (as far as possible with a limited mesh resolution), the solution with a resolved shear layer converges to the Myers boundary condition.

A more (2 point) or less (10 point) aggressive filtering of the convective and curvature terms is also straight forward to implement with a Myers boundary condition. Some results are presented in Figure 8. As can be seen, even the more aggressive filter has no significant impact on the acoustic solution, apart from making it stable for long term simulation.

5 Conclusions

Application of Impedance Models for Turbomachinery Noise

From the above consideration, the following conclusions can be drawn for turbomachinery noise going from the most demanding computational methods to the methods with the highest number of modeling assumptions:

- Direct numerical simulation of an orifice under grazing flow [20] will help to improve the understanding of impedance and it will help the development of impedance models in the future by extending the understanding from grazing flow experiments with samples. However, the cost of this simulations make this method completely infeasible for the simulation of turbomachinery noise.
- Modern aeroengine designs raise more and more the requirement for impedance models in CFD methods, as the acoustic lining is applied in the source region as well. This requirement may be fulfilled by time domain impedance models, rather than a resolution of the liner cells for the moment. An example for such implementation has been demonstrated in [19]. Also hybrid approaches are thinkable, where the resistance of the facing sheet of a liner is modeled by its pressure drop, whereas the flight time for the reflected wave is calculated by a resolved 1D cell (without walls) behind the facing sheet, in this way removing the need of a storage term. The Myers boundary condition is not required, because the shear layers are resolved and non-slip conditions are applied for the velocity components parallel to the wall, whereas the normal component is determined from the impedance model.
- Especially for rotating components, linearized Navier Stokes formulations in the frequency domin have been developed for CFD applications (e.g. [19] and commercial solutions). These formulations can directly make use of the impedance in the frequency domain.
- For finer meshes in CAA, the step to a resolved, or at least approximate boundary layer profile in the base flow seems unavoidable for CAA simulations. Such high fidelity CAA simulations would provide all important features of the sound propagation and will only be applicable for some computations to understand the physics of sound propagation in a specific case.
- For time domain CAA simulations, the impedance boundary conditions based on the Myers boundary condition are only applicable, if the grid resolution is low. In turbomachinery applications, this will be an early design phase or automatized design optimization with time domain methods.
- Finally frequency domain noise prediction methods and boundary element methods still provide fast and robust prediction tools with the possibility to include impedance.

Acknowledgments

The author would like to acknowledge the support of the Rolls-Royce Deutschland LTD & Co KG.

References

[1] U. Ingard. “Influence of fluid motion past a plane boundary on sound reflection, absorption, and transmission.” Journal of the Acoustical Society of America, 31(7), 1035–1036. 1959.

[2] M. K. Myers. “On the acoustic boundary condition in the presence of flow.” Journal of Sound and Vibration, 71(8), 429–434. 1980.

[3] J.W. Kooi and S. L. Sarin. “An Experimental Study of the Acoustic Impedance of Helmholtz Resonator Arrays Under a Turbulent Boundary Layer.” AIAA Paper 1981–1998. 1981.

[4] M. G. Jones, T. L. Parrott, and W. R. Watson. “Comparison of Acoustic Impedance Eduction Techniques for Locally-Reacting Liners.” AIAA Paper 2003–3306. 2003.

[5] M. G. Jones, W. R. Watson, M. B. Tracy, and T. L. Parrott. “Comparison of Two Waveguide Methods for Educing Liner Impedance in Grazing Flow.” AIAA Journal, 42(2), 232–240. 2004.

[6] M. G. Jones, W. R. Watson, and T. L. Parrott. “Comprehensive Benchmark Data for Evaluation of Aeroacoustic Propagation Codes with Grazing Flow.” AIAA Paper 2005–2853. 2005.

[7] S. Busse, C. Richter, F. Thiele, C. Heuwinkel, L. Enghardt, I. Röhle, U. Michel, P. Ferrante, and A. Scofano. “Impedance Deduction Based on Insertion Loss Measurements of Liners under Grazing Flow Conditions.” AIAA Paper 2008–3014. 2008.

[8] Walter Eversman and Judith Gallman “Impedance Eduction with an Extended Search Procedure” AIAA Journal 49(9), 1960-1970, 2011, doi: 10.2514/1.55695

[9] T. Zandbergen “Are locally reacting acoustic liners always behaving as they should” AIAA Paper 1979-567, 1979.

[10] C. Richter, F. Thiele, X. D. Li, and M. Zhuang. “Comparison of Time-Domain Impedance Boundary Conditions for Lined Duct Flows.” AIAA Journal, 45(6), 1333–1345. 2007.

[11] A. Scofano, P. B. Murray, and P. Ferrante. “Back-Calculation of Liner impedance using Duct Insertion Loss Measurements and FEM Predictions.” AIAA Paper 2007–3534. 2007.

[12] C. K. W. Tam and L. Auriault. “Time-Domain Impedance Boundary Conditions for Computational Aeroacoustics.” AIAA Journal, 34(5), 917–923. 1996.

[13] Y. Özyörük and L. N. Long. “A time-domain implementation of surface acoustic impedance condition with and without flow.” AIAA Paper 1996–1663. 1996.

[14] Y. Özyörük, L. N. Long, and M. G. Jones. “Time-domain numerical simulation of a flow-impedance tube.” Journal of Computational Physics, 146(1), 29–57. 1998.

[15] Y. Özyörük and L. N. Long. “Time-domain calculation of sound propagation in lined ducts with sheared flows.” AIAA Journal, 38(5), 768–773. 2001.

[16] K.-Y. Fung, H. B. Ju, and B. Tallapragada. “Impedance and its time-domain extensions.” AIAA Journal, 38(1), 30–38. 2000.

[17] S. W. Rienstra. “Impedance Models in Time Domain, Including the Extended Helmholtz Resonator Model.” AIAA Paper 2006–2686. 2006.

[18] N. Chevaugeon, J.-F. Remacle, and X. Gallez. “Discontinous Galerkin Implementation Of The Extended Helmholtz Resonator Model In Time Domain.” AIAA Paper 2006–2569. 2006.

[19] M. O. Burak, M. Billson, L.-E. Eriksson, and S. Baralon. “Validation of a Time & Frequency Domain Grazing Flow Acoustic Liner Model.” AIAA Journal, 47(8), 1841–1848. 2008.

[20] Qi Zhang and Daniel J. Bodony “Numerical investigation and modelling of acoustically excited flow through a circular orifice backed by a hexagonal cavity” Journal of Fluid Mechanics 693, 367-401, 2012.

[21] Qi Zhang and Daniel J. Bodony “Numerical Simulation of Two-Dimensional Acoustic Liners with High-Speed Grazing Flow”, AIAA Journal, vol. 49, issue 2, pp. 365-382.

[22] E. J. Brambley and N. Peake. “Classification of aeroacoustically relevant surface modes in cylindrical lined ducts.” Wave Motion, 43, 301–310. 2006.

[23] S.W. Rienstra and G. G. Vilenski. “Spatial Instability of Boundary Layer Along Impedance Wall.” AIAA Paper 2008–2932. 2008.

[24] E. J. Brambley and N. Peake. “Stability and acoustic scattering in a cylindrical thin shell containing compressible mean flow.” Journal of Fluid Mechanics, 602, 403–426. 2008.